# MEMS 2-Bit Phase-Shifter Failure Mode and Reliability Considerations for Large $X$-Band Arrays

Joseph G. Teti, Jr., *Senior Member, IEEE,* and Francis P. Darreff, *Member, IEEE,*

***Abstract*—RF microelectromechanical systems (MEMS) switch technology used in the fabrication of phase-shifter circuits is examined from the perspective of failure mode and reliability implications on the performance of large $X$-band array antennas. Amplitude and phase-state failure probability density functions (pdfs) conditioned on switch probability of failure are formulated for both the hybrid-T (switched line) and coupled-line phase-shifter circuit topologies. The pdfs are used to assess the phase-shifter failure impact on overall array level performance in terms of gain loss and the increase in rms sidelobe level. Reliability and lifetime implications are addressed through considering a probability of switch failure that increases with cycling. The phase-shifter lifetime switching considerations are related to radar system lifetime beam switching requirements consistent with plausible radar system applications. The key findings are that RF MEMS switch mean time to failure ~125 000 h or longer, consistent with ~100–125 phase-shifter state switches per second (~ $10^{11}$ switch operations), are reasonable expectations for RF MEMS phase-shifter technology to meet in order to be considered viable for a broad range of array antenna applications.**

***Index Terms*—Microelectromechanical systems (MEMS) phase-shifter failure, MEMS phase-shifter lifetime, MEMS phase-shifter reliability, RF MEMS, $X$-band MEMS 2-bit phase shifters.**

## I. INTRODUCTION

THE application of microelectromechanical systems (MEMS) switch technology in the fabrication of phase-shifter circuits has been described extensively in the open literature (e.g., [1]–[6]). MEMS technology for RF applications continues to mature as the understanding for the device physics improves. In addition, circuit fabrication and packaging techniques that are both suitable for low-cost manufacturing and realizing long-term reliable operation are essential for widespread adoption in system applications. Among the attractive potential advantages of MEMS phase shifters compared to competing technologies are reduced power consumption, size, weight, and cost. When combined with integrated RF manufacturing techniques, MEMS phase-shifter technology has the potential to allow the production of large-scale array antennas at considerably reduced costs compared to competing technologies [3], [5]. Furthermore, RF MEMS switch technology could prove to be a performance and cost enabler for large lightweight array antenna systems. However, for the benefits of MEMS phase-shifter technology to be realized, the reliability and lifetime characteristics of the technology must meet the requirements of the intended antenna system application.

This paper examines the reliability and lifetime requirements of 2-bit MEMS phase shifters for large $X$-band array antenna systems (e.g., $\geq\ 10\ \mathrm{m}^2$) through the consideration of failure modes for the common hybrid-T and coupled line phase-shifter circuit topologies [7]. Note that other types of MEMS phase-shifter topologies (e.g., lumped element, star, etc.) have also been reported, but the hybrid-T and coupled-line phase-shifter circuit topologies were chosen not only because they are considered to be very common, but because they have been extensively implemented with diode switches. A single MEMS switch-failure mode known as "stiction" is considered exclusively in characterizing phase-shifter failure modes. The term "stiction" describes the phenomena of the switch remaining closed after actuation, and is generally believed to be the predominant failure condition. While other MEMS switch-failure modes are known,[1] the exclusive consideration of stiction is useful to develop a baseline on MEMS switch reliability and lifetime requirements. The analysis formulates amplitude and phase-state failure probability density functions (pdfs) conditioned on switch probability of failure for each phase-shifter circuit topology. The pdfs are used to assess the phase-shifter failure impact on overall array level performance in terms of gain loss and the increase in rms sidelobe level. Reliability and lifetime implications are addressed through considering a probability of switch failure that increases with cycling. The phase-shifter lifetime switching considerations are related to radar system lifetime beam-switching requirements consistent with plausible applications.

## II. PHASE-SHIFTER CIRCUIT TOPOLOGY OVERVIEW AND FAILURE MODES

### A. Coupled Line

An implementation of a coupled-line phase-shifter circuit topology is illustrated in Fig. 1 for an $X$-band 2-bit phase

Manuscript received July 8, 2003; revised September 14, 2003. This work was supported in part by the Special Projects Office of the Defense Advanced Research Projects Agency through the Air Force Research Laboratory Contract F30602-97-D-0070.

The authors are with Lambda Science Inc., Wayne, PA 19087 USA (e-mail: jgteti@lamsci.com; fpdarreff@lamsci.com).

Digital Object Identifier 10.1109/TMTT.2003.822017

---

[1] MEMS switch fail open conditions can also occur from other failure mechanisms such as dielectric charging for the capacitive-shunt type switch, and contact resistance buildup for the metal-to-metal type switch, which, for both switch types, are brought about gradually from switch cycling. Unfortunately, treatment of these and other types of failure mechanisms was limited by insufficient or unavailable measurement data at the time this study was performed.

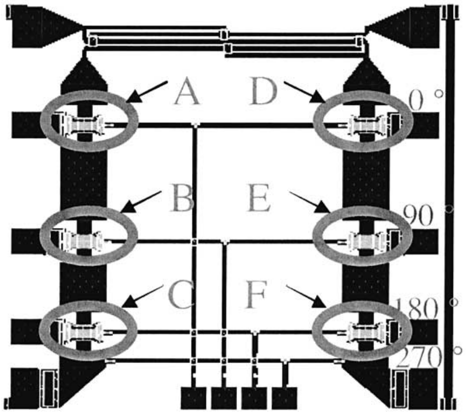

(a)

| | A | B | C | D | E | F |
|---|---|---|---|---|---|---|
| **0** | 1 | 1 | 1 | 1 | 1 | 1 |
| **9 0** | 0 | 1 | 1 | 0 | 1 | 1 |
| **1 8 0** | 0 | 0 | 1 | 0 | 0 | 1 |
| **2 7 0** | 0 | 0 | 0 | 0 | 0 | 0 |

**1 - Switch down**
**0 - Switch up**

(b)

Fig. 1. (a) Coupled-line phase-shifter circuit topology. (b) State description [4].

shifter. The operating characteristics and measured performance of the coupled line 2-bit phase-shifter circuit topology shown in Fig. 1 are reported in [4]. Fig. 1(a) indicates the location of the MEMS single-pole single-throw (SPST) switches, and Fig. 1(b) describes the switching logic. The 2-bit topology considered consists of six switches that are controlled in pairs to set the device state. As indicated in the switching logic description, pairs of switches are opened to select the appropriate coupled line length. Fig. 2(a) describes the phase-shifter performance for proper operation, and Fig. 2(b) summarizes the phase-shifter failure modes for switches failed in the closed position. Inspection of Fig. 2(b) indicates that some failure modes are more severe than others, and the impact is different for different phase states. Failure mode cases indicating more than 3-dB loss are shown italicized, suggesting somewhat arbitrarily that these failure conditions could be considered more severe, perhaps distinguishing "hard" failures from "soft" failures. However, note that this interpretation can be misleading in the sense that radiating with the wrong phase is more detrimental than attenuating at this device state unless the failed phase state happens to match the desired array scan conditions.

| Setting (°) | Amp (dB) | Phase (°) |
|---|---|---|
| 0 | 0.59 | 0.0 |
| 90 | 0.92 | 99.3 |
| 180 | 0.86 | 180.6 |
| 270 | 0.58 | 247.3 |

(a)

| | Setting (°) | Amp (dB) | Phase (°) |
|---|---|---|---|
| "A" Stuck | 0 | * | * |
| | 90 | *3.6* | -50.9 |
| | 180 | *13.7* | -77.8 |
| | 270 | *6.8* | -51.7 |
| "B" Stuck | 0 | * | * |
| | 90 | * | * |
| | 180 | 2.4 | -40.5 |
| | 270 | *7.3* | -61.0 |
| "C" Stuck | 0 | * | * |
| | 90 | * | * |
| | 180 | * | * |
| | 270 | 1.7 | -32.7 |

*** No Change**

(b)

Fig. 2. (a) Coupled-line phase-shifter normal operation. (b) Failure-mode characteristics (courtesy of the Raytheon Systems Company, Dallas, TX).

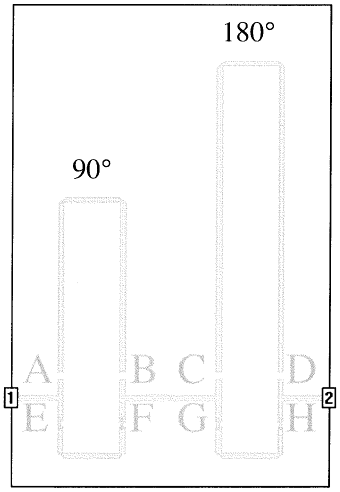

(a)

| | A | B | C | D | E | F | G | H |
|---|---|---|---|---|---|---|---|---|
| **0** | 0 | 0 | 0 | 0 | 1 | 1 | 1 | 1 |
| **9 0** | 1 | 1 | 0 | 0 | 0 | 0 | 1 | 1 |
| **1 8 0** | 0 | 0 | 1 | 1 | 1 | 1 | 0 | 0 |
| **2 7 0** | 1 | 1 | 1 | 1 | 0 | 0 | 0 | 0 |

**1 - Switch down**
**0 - Switch up**

(b)

Fig. 3. (a) Hybrid-T phase-shifter circuit topology (motivated by [8]). (b) State description.

### *B. Hybrid T*

An idealized hybrid-T phase-shifter circuit topology is illustrated in Fig. 3 for a 2-bit phase shifter. The hybrid-T 2-bit phase-shifter circuit topology is motivated by the 4-bit phase-shifter circuit topology in [8]. Fig. 3(a) indicates the location of the MEMS SPST switches, and Fig. 3(b) describes the switching logic. The 2-bit topology considered consists of eight switches that are controlled in pairs to set the device state. The switching logic description indicates that adjacent pairs of switches are operated in a complementary fashion to switch in or out the desired line lengths. An $X$-band circuit model was constructed to calculate proper operation- and failure-mode performance, and the results are summarized in Fig. 4. Fig. 4(a) illustrates insertion loss and phase-delay performance for the case of all switches operating properly. Fig. 4(b) illustrates failure-mode performance characteristics for all possible switch-failure combinations. Inspection of Fig. 4(b) suggests that many of the failure modes

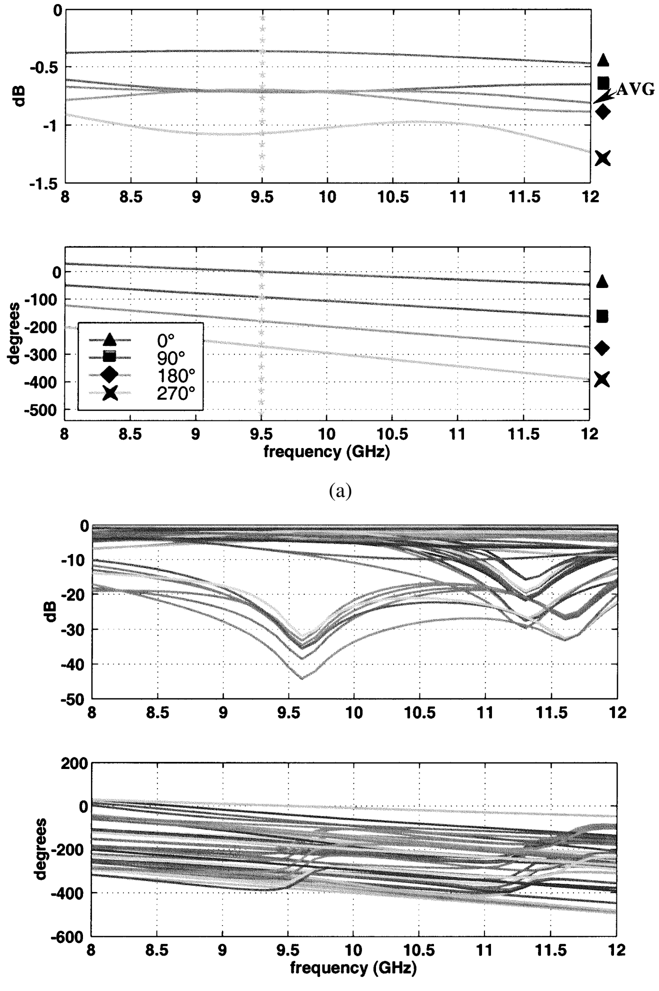

(a)

(b)

Fig. 4. (a) Hybrid-T phase-shifter normal operation. (b) Failure-mode characteristics.

could be considered as soft versus hard failures, where hard failures could be arbitrarily associated with loss conditions that exceed 3 dB, which is consistent with the coupled-line criteria. However, the same cautionary consideration noted for the coupled-line topology applies.

## III. FAILURE-MODE CONDITIONAL STATISTICS

The failure-mode characteristics summarized in Section II serve as a basis for developing a statistical description of phase-shifter failure modes conditioned on the probability of a single switch failure. In the results that follow, it is assumed that all phase-shifter states are equally likely.

### A. Coupled Line

Formulating the conditional statistics for the coupled-line phase-shifter topology begins with observing that

$$P(\geq 1 \text{ switch failure}) = P(F) = 1-(1-p)^6 \tag{1}$$

where $p$ is the probability of an individual switch failure. Furthermore, inspection of Fig. 2 indicates that the probability of

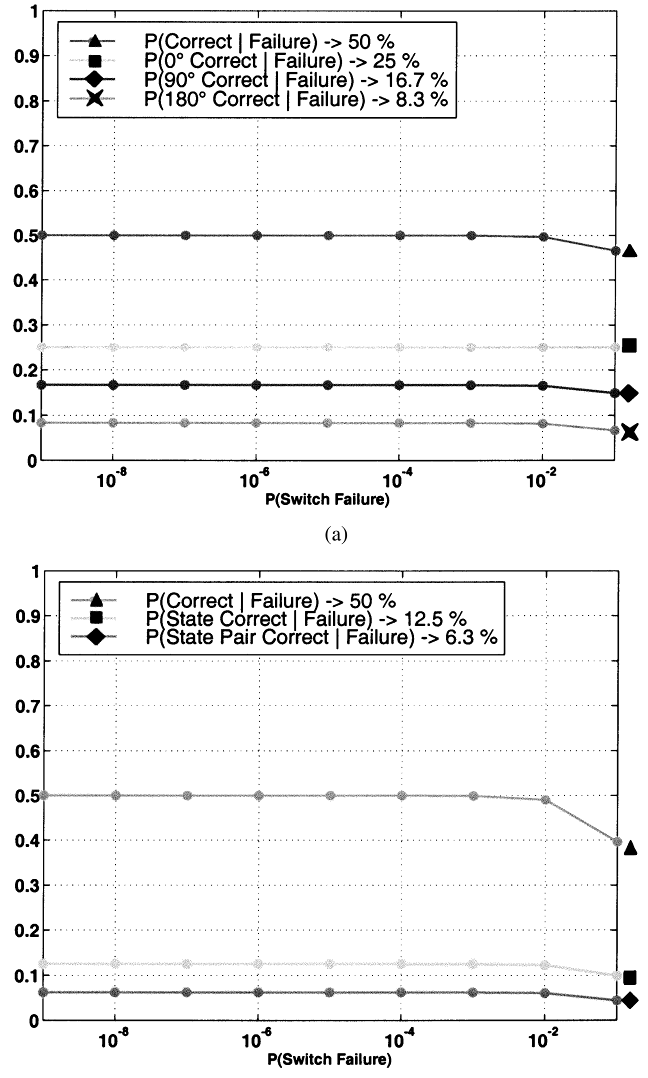

(a)

(b)

Fig. 5. (a) Coupled line. (b) Hybrid-T failure-mode overview.

correct phase-shifter states under failure-mode conditions are given by

$$\begin{aligned} &P\big(\{0^\circ\}\text{correct}|F\big)\\ &\quad = 0.25 \end{aligned} \tag{2a}$$

$$\begin{aligned} &P\big(\{90^\circ\}\text{correct}|F\big)\\ &\quad = \frac{p(1-p)^5+1.5\,p^2(1-p)^4+p^3(1-p)^3+0.25\,p^4(1-p)^2}{1-(1-p)^6}\\ &\quad = P\big(\{0^\circ,90^\circ\}\text{correct}|F\big) \end{aligned} \tag{2b}$$

$$\begin{aligned} &P\big(\{180^\circ\}\text{correct}|F\big)\\ &\quad = \frac{0.5\,p(1-p)^5+0.25\,p^2(1-p)^4}{1-(1-p)^6}\\ &\quad = P\big(\{0^\circ,90^\circ,180^\circ\}\text{correct}|F\big) \end{aligned} \tag{2c}$$

where the probability of incorrect states resulting from failed switches is given by

$$\begin{aligned} P(\text{mistake}|F) &= 1-P(\text{correct}|F)\\ &= 1-\Big(P\left(\{0^\circ\}\text{correct}|F\right)\\ &\qquad + P\big(\{90^\circ\}\text{correct}|F\big)\\ &\qquad + P\big(\{180^\circ\}\text{correct}|F\big)\Big). \end{aligned} \tag{3}$$

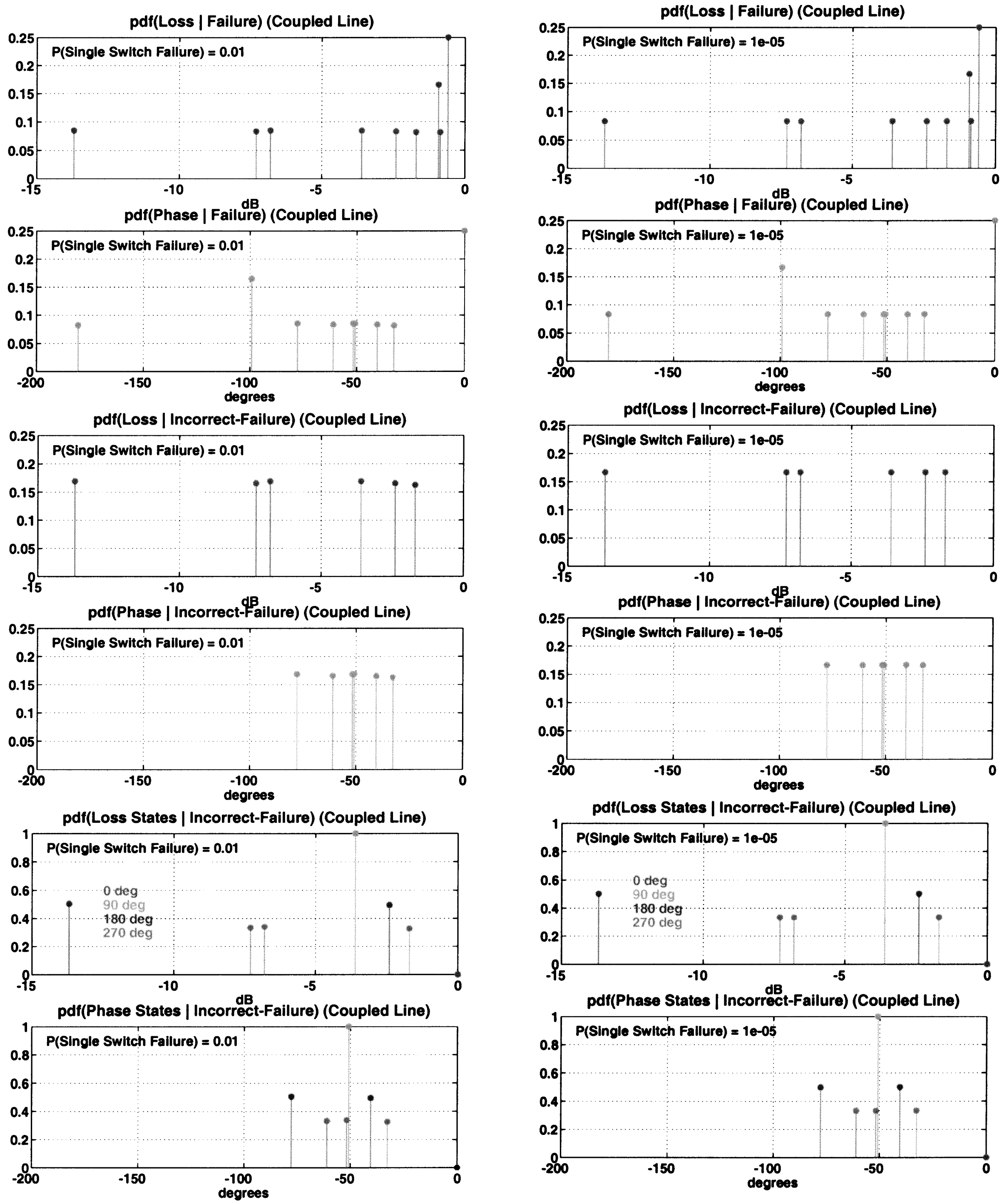

(a) (b)

Fig. 6. Coupled-line failure pdfs. (a) $p = 10^{-2}$. (b) $p = 10^{-5}$

Note that the 0° phase state for the coupled-line circuit topology is never lost, as indicated by the fact that (2a) is independent of the probability of an individual switch failure $p$. Equation (2) probabilities are illustrated in Fig. 5(a), where the asymptotic probabilities for being correct for 90° and 180° phase states are 16.7% and 8.3%, respectively [see (2b) and (2c)]. Fig. 5(a) also illustrates that there is a 50% probability of being correct under all possible switch-failure combinations when asymptotic conditions are met. The asymptotic conditions (observed for $p \leq 10^{-4}$) are expected since

$$\begin{aligned} P(\text{state failure}) &= P(\text{state failure}| \geq 1 \text{ switch failure}) \\ &\quad \times P(\geq 1 \text{ switch failure}) \\ &\xrightarrow{p\leq 10^{-4}} \left(\frac{1}{2}\right)\left\{1-(1-p)^6\right\}. \end{aligned} \tag{4}$$

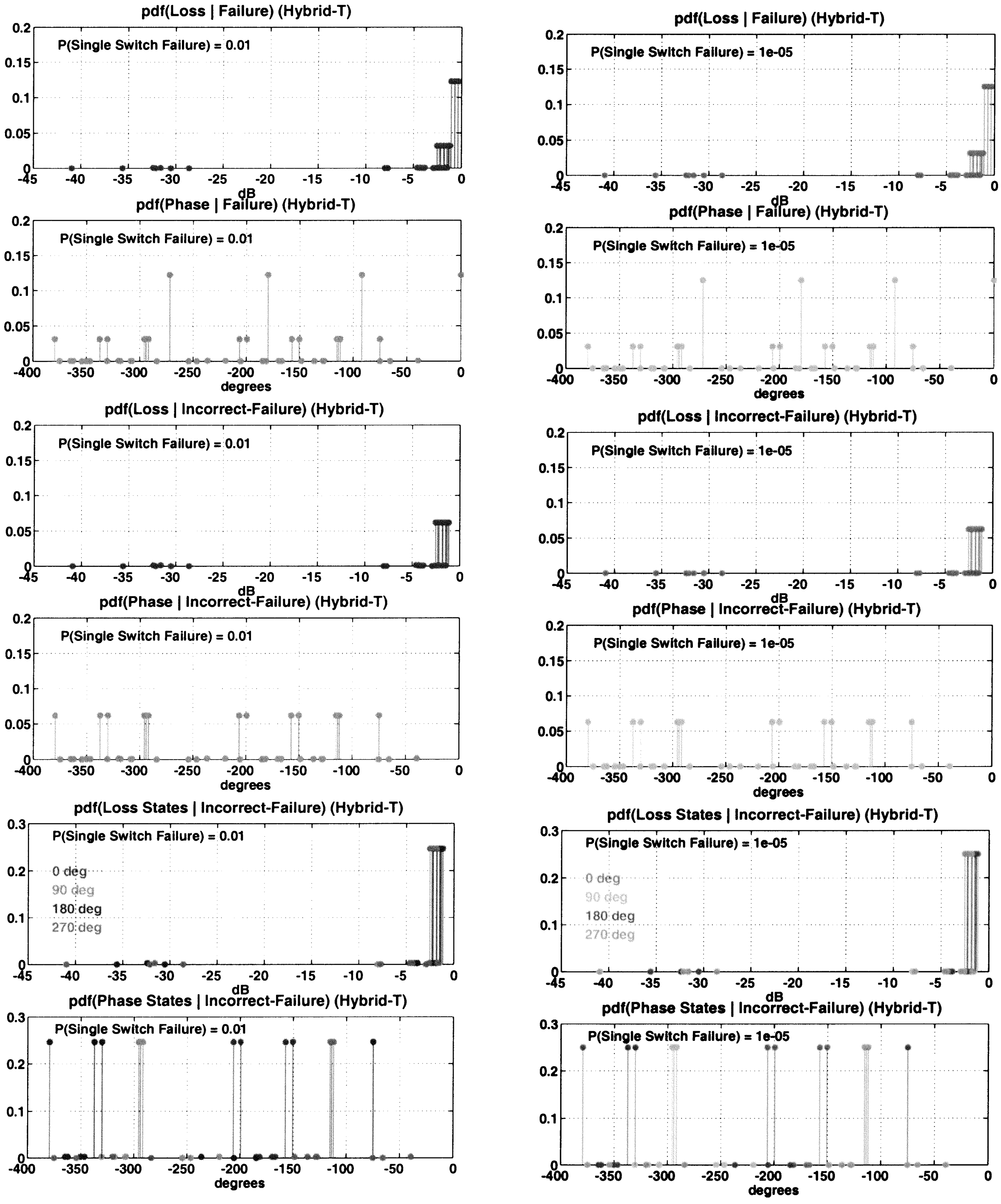

(c) (d)

Fig. 6. *(Continued.)* Hybrid-T failure pdfs. (c) $p = 10^{-2}$. (d) $p = 10^{-5}$.

Although (1)–(4) are useful as a starting point in gaining insight into the nature of phase-shifter failure-mode implications, a complete statistical description is needed to complete an assessment of the performance impact at the array level. Consequently, a pdf has been constructed that accounts for the combinatorial possibilities of individual switch failures. Writing expressions for the combinatorial possibilities and integrating (marginalizing) appropriately, results in the pdf descriptions presented in Fig. 6(a)–(d) for two different switch-failure probabilities. Specifically, results are shown for $p = 10^{-2}$ and $p = 10^{-5}$ to demonstrate consistency with the asymptotic results shown in Fig. 5(a).

## *B. Hybrid T*

Following the same procedure used for the coupled-line phase shifter, the conditional failure statistics for the hybrid-T phase-shifter topology begins with the failure probability

$$P(\geq 1 \text{ switch failure}) = P(F) = 1 - (1 - p)^8. \qquad (5)$$

Examination of the state description in Fig. (3) indicates that the probability of correct phase-shifter states under failure-mode conditions are given by

$$\begin{aligned} &P\big(\{0^\circ\}\text{correct}|F\big)\\ &\quad= \frac{p(1-p)^7+1.5\,p^2(1-p)^6+p^3(1-p)^5+0.25\,p^4(1-p)^4}{1-(1-p)^8}\\ &\quad= P\big(\{90^\circ\}\text{correct}|F\big)\\ &\quad= P\big(\{180^\circ\}\text{correct}|F\big)\\ &\quad= P\big(\{270^\circ\}\text{correct}|F\big) \qquad \text{(6a)}\\ &P\big(\{0^\circ,90^\circ\}\text{correct}|F\big)\\ &\quad= \frac{0.5\,p(1-p)^7+0.25\,p^2(1-p)^6}{1-(1-p)^8}\\ &\quad= P\big(\{0^\circ,180^\circ\}\text{correct}|F\big)\\ &\quad= P\big(\{90^\circ,270^\circ\}\text{correct}|F\big)\\ &\quad= P\big(\{180^\circ,270^\circ\}\text{correct}|F\big) \qquad \text{(6b)} \end{aligned}$$

where the probability of incorrect states resulting from failed switches is given by

$$\begin{aligned} P(\text{mistake}|F) &= 1 - P(\text{correct}|F)\\ &= 1 - \Big(4P\big(\{0^\circ\}\text{correct}|F\big)\Big). \end{aligned} \tag{7}$$

Note that (6a) indicates that the probability of individual phase states being correct are equal given switch failures are present. In addition, (6b) indicates that specific pairs of phase states being correct also share equal probabilities in the presence of switch failures. Equation (6) probabilities are illustrated in Fig. 5(b), where the asymptotic probabilities for being correct for a single phase state and state pair are 12.5% and 6.3%, respectively [see (6a) and (6b)]. Fig. 5(b) also illustrates that there is a 50% probability of being correct under all possible switch-failure combinations when asymptotic conditions are met. The hybrid-T phase-shifter result for 50% probability of being correct is the combination of correct single-phase-state results. Note that the state pair cases are comprised of outcomes that are already included in the single-state probabilities. As in the case of the coupled-line phase-shifter topology, the hybrid-T asymptotic conditions (observed for $p \leq 10^{-4}$) are expected since

$$\begin{aligned} P(\text{state failure}) &= P(\text{state failure}|\geq 1 \text{ switch failure})\\ &\quad\times P(\geq 1 \text{ switch failure})\\ &\xrightarrow{p\leq 10^{-4}} \left(\frac{1}{2}\right)\left\{1-(1-p)^8\right\}. \end{aligned} \tag{8}$$

Accounting now for all possible combinatorial possibilities of individual switch failures, a pdf for the hybrid-T phase shifter has been constructed using the same approach used in constructing the pdf for the coupled line phase shifter. The pdf descriptions of hybrid-T failures are included in Fig. 6(a)–(d) for $p = 10^{-2}$ and $p = 10^{-5}$ to demonstrate consistency with the asymptotic results shown in Fig. 5(b). Note that operation at 9.5 GHz [indicated by the vertical line in Fig. 4(a)] is used to assess array-level performance for the hybrid-T circuit topology.

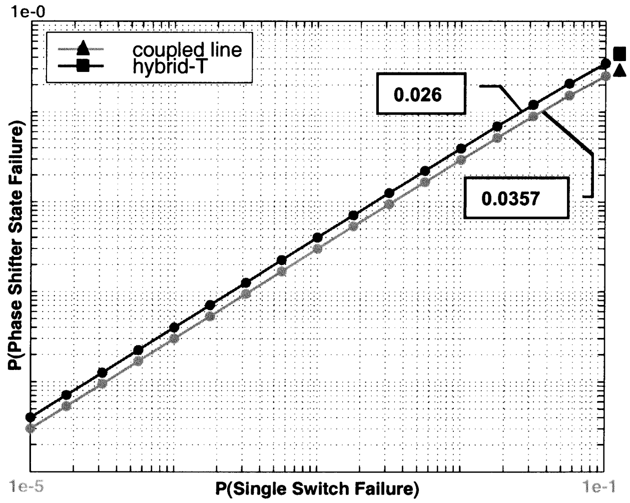

Fig. 7. Probability relation between phase-state and switch failures.

The pdf descriptions of the type shown in Fig. 6(a)–(d) facilitate direct calculation of the probability relation between the phase-shifter state failures and switch failures. The relationship is given in Fig. 7 for both the coupled-line and hybrid-T phase-shifter circuit topologies. Not surprising, the hybrid T has a slightly higher probability of phase-state failure for a given probability of switch failure due to the greater number of switches in the circuit topology.

## IV. ARRAY-LEVEL PERFORMANCE

Failure-mode pdfs conditioned on the switch probability of failure of the type illustrated in Fig. 6(a)–(d) are used to compute the second-order statistics of the amplitude and phase errors corresponding to the state failures. In addition, second-order statistics for proper phase-shifter operation are computed in a similar fashion. The variance of the errors caused by switch failures are combined with the variances for proper operation (e.g., quantization) according to $\sigma_T^2 = \sigma_{T|\text{Fail}}^2 P(F) + \sigma_{T|\text{No Fail}}^2(1-P(F))$, where $\sigma_T^2 = \sigma_A^2 + \sigma_\theta^2$ denotes the total variance. Using the total error variance directly, the array antenna gain loss and the increase in rms sidelobe level (in decibels) are given by $G_{\text{loss}} = 10\log(1-\sigma_T^2)$ and $SLL_{\text{rms}} = 10\log(\sigma_T^2/N(1-\sigma_T^2))$, respectively, where $N$ is the total number of array elements. Fig. 8 summarizes results for both the coupled-line and hybrid-T phase-shifter circuit topologies. The array failure analysis results for the increase in rms sidelobe level are shown relative to 2-bit quantization performance. Note that the results shown for the coupled-line and hybrid-T phase-shifter circuit topologies only differ in the correspondence between the device state and the switch probability of failures (see Fig. 7).

## V. RELIABILITY AND LIFETIME CONSIDERATIONS

The results of Section IV quantify the impact of MEMS switch and phase-shifter phase-state failures on overall array performance with respect to gain loss and rms sidelobe level increase. Accordingly, the relation to reliability and lifetime requirements is now established. A probability of switch failure that increases with cycling is considered, where a notional

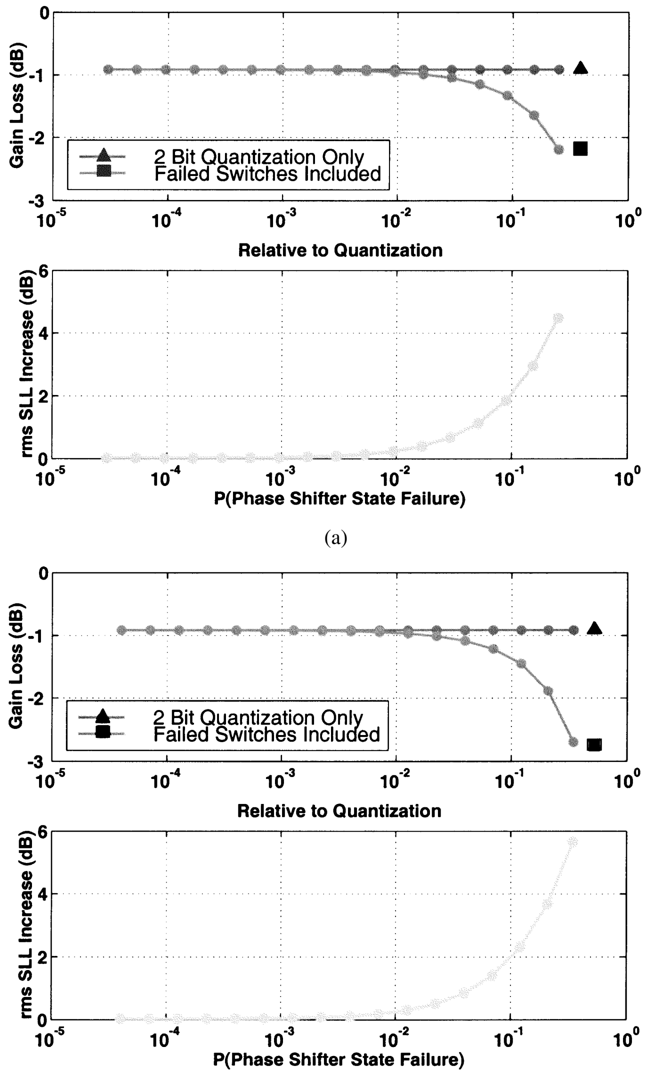

(a)

(b)

Fig. 8. Array gain loss and degraded rms sidelobe level. (a) Coupled line. (b) Hybrid T.

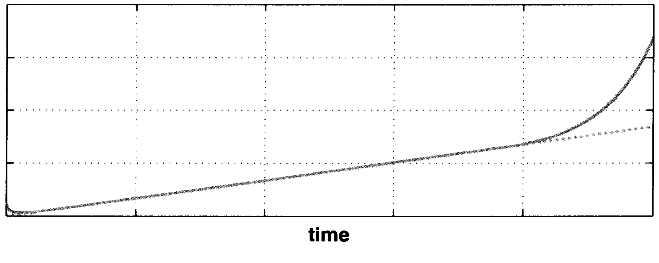

Fig. 9. RF MEMS switch-failure-rate model (failure probability increasing with cycling).

failure rate is illustrated in Fig. 9. The failure-rate description shown in Fig. 9 is basically comprised of three regions consisting of infant mortality, gradual (normal) accumulation of failures, and the accelerated accumulation of failures that might be expected with impending end-of-life failure characteristics. Fig. 9 also includes an approximate linear description of the failure rate that matches in the region considered to describe the normal accumulation of failures. Under failure-rate conditions that are well represented by a linear description, the

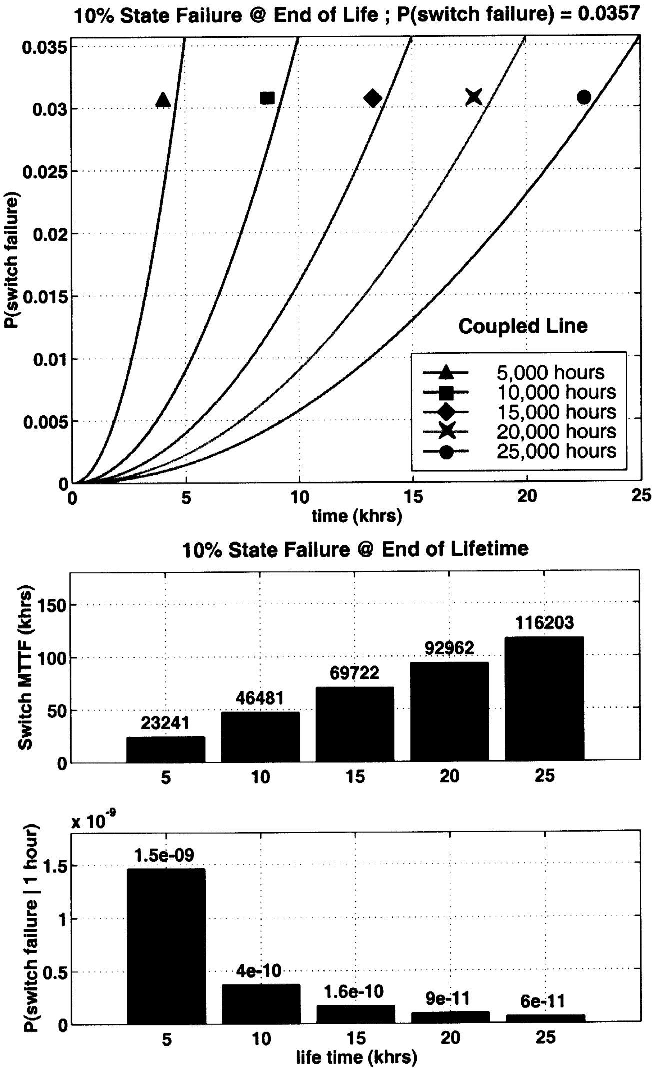

(a)

Fig. 10. Reliability and lifetime considerations. (a) Coupled line.

corresponding reliability and lifetime statistics are given by the well-known Rayleigh failure-rate description. Hence, the failure rate is given by $y(t) = -Y'(t)/Y(t) = \mu t$ with lifetime described by $P(t_{\text{life}} > t) = \exp\{-0.5\ \mu t_{\text{life}}^2\}$, and mean time to failure (MTTF) $= \sqrt{\pi/2\mu}$. In order to proceed, a degraded acceptable end-of-life performance for the array needs to be considered in combination with array antenna lifetime that is suitable for system applications. Consideration of large $X$-band array antenna system applications leads to the desire for 5000–25 000 h of operational lifetime capability, which is consistent with ~100–125 phase-shifter state switches per second. Assuming acceptable degraded end-of-life array performance, relative quantization allows for <1 dB of gain loss and ~2 dB increase in rms sidelobe level. Fig. 8 suggests that 10% phase-shifter state failures represent reasonable end-of-life operating conditions. Using the prescribed conditions, Fig. 10(a) and (b) summarizes failure-rate and lifetime considerations for the coupled-line and hybrid-T phase-shifter circuit topologies. The results correspond to 10% state failure at the end of life represented as a function of switch-failure probability. The switch-failure probability conditions can be

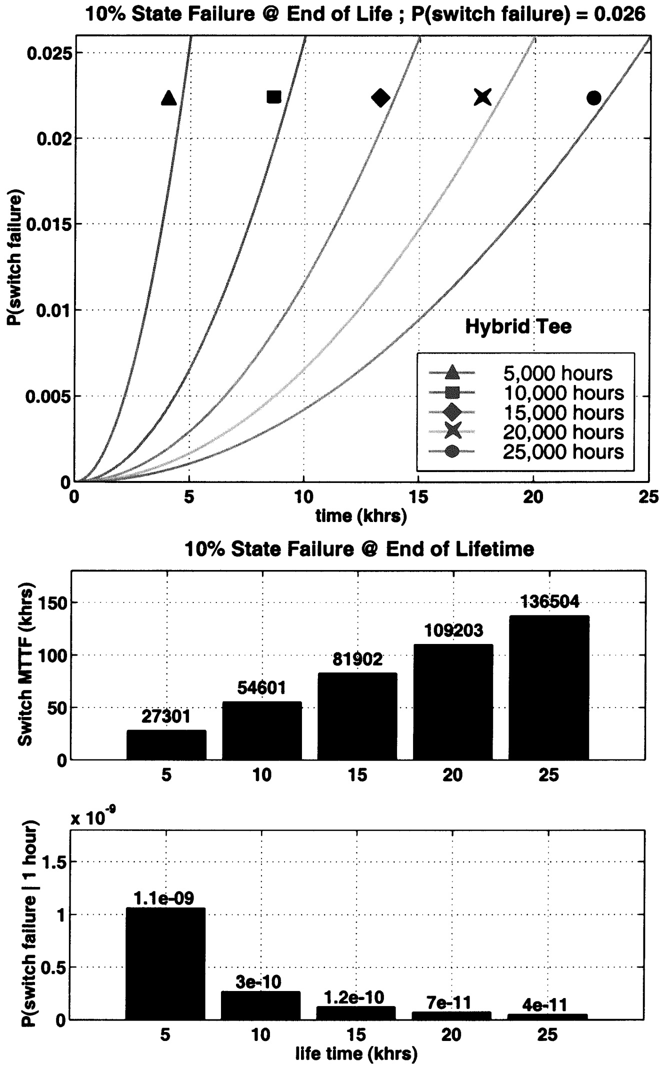

(b)

Fig. 10. *(Continued.)* Reliability and lifetime considerations. (b) Hybrid T.

verified from Fig. 7. Note that the results are a factor of two conservative with any single switch closure occurring for 50% of the state conditions. A comparison of the failure-rate and lifetime results for the two phase-shifter circuit topologies indicates that the hybrid-T circuit topology requires slightly higher switch reliability, as evidenced by ~17% longer MTTF required to satisfy the prescribed 10% failure end-of-life conditions. The higher switch reliability requirement for the hybrid-T phase shifter is primarily due to the greater number of switches and the relation between switch and state failures (see Fig. 7). Not withstanding this minor distinction, the switch reliability and lifetime requirements are very similar for the two circuit topologies. More importantly, switch MTTFs ~125 000 h or longer, consistent with ~100–125 phase-shifter state switches per second, appear to represent reasonable reliability and lifetime expectations for RF MEMS phase-shifter technology to be a candidate for a broad range of array antenna applications.

## VI. CONCLUSIONS

The application of RF MEMS switch technology to phase-shifter design and fabrication has the potential to yield reduced power consumption, size, weight, and cost compared to competing technologies (e.g., diodes). Furthermore, the favorable attributes of RF MEMS phase-shifter technology could prove to be a performance and cost enabler for extremely large array antenna systems. However, the reliability and lifetime of RF MEMS switches is a concern. This effort was undertaken to assess the impact of RF MEMS phase-shifter failure modes on large $X$-band array antennas (e.g., $\geq$ 10 m$^2$), and relate performance degradation to reliability and lifetime requirements. The utilization of RF MEMS switches in the design and fabrication of 2-bit phase shifters were considered for both the hybrid-T (switched line) and coupled-line phase-shifter circuit topologies. Conditional statistics describing the failure modes for each circuit topology were developed to assess the impact of phase-shifter failure on overall array level performance in terms of gain loss and rms sidelobe level increase. The results indicate that similar performance degradation can be expected with either circuit topology under reasonably acceptable operating conditions. Less than 1-dB gain loss and ~2-dB increase in the rms sidelobe level was adopted to represent acceptable degraded end-of-life array performance with 10% phase-shifter state failures. The probability of a switch failure was considered to increase linearly with cycling under normal operating conditions consistent with a Rayleigh failure-rate description. Reliability and lifetime considerations for 10% end-of-life failure conditions indicate that RF MEMS switch MTTFs ~125 000 h or longer, consistent with ~100–125 phase-shifter state switches per second (~10$^{11}$ switch operations), are required. These reliability and lifetime requirements are reasonable expectations for RF MEMS phase-shifter technology to meet in order to be considered viable for a broad range of array antenna applications. While the reliability and lifetime conclusions are based exclusively on stiction as the failure condition, the inclusion of other failure mechanisms leading to MEMS switch fail open conditions are not believed to have a significant impact on these conclusions.

## ACKNOWLEDGMENT

The authors thank the Raytheon Systems Company, and, in particular, A. Malczewski, for allowing the use and publication of the coupled line phase-shifter measurement results shown in Fig. 2, and C. Caddel and C. L. Goldsmith for help with obtaining public release.

## REFERENCES

[1] E. R. Brown, "RF-MEMS switches for reconfigurable integrated circuits," *IEEE Trans. Microwave Theory Tech.*, vol. 46, pp. 1868–1880, Nov. 1998.
[2] N. S. Barker and G. M. Rebeiz, "Distributed MEMS true-time delay phase shifters and wide-band switches," *IEEE Trans. Microwave Theory Tech.*, vol. 46, pp. 1881–1890, Nov. 1998.
[3] W. R. Norvell, R. L. Hancock, J. K. Smith, M. L. Pugh, S. W. Theis, and J. Kviatkofsky, "Micro-mechanical switch (MEMS) technology applied to electronically scanned arrays for space based radar," in *Proc. IEEE Aerospace Conf.*, vol. 3, Aspen, CO, Mar. 6–13, 1999, pp. 239–247.
[4] A. Malczewski, S. Eshelman, B. Pillans, J. Ehmke, and C. L. Goldsmith, "$X$-band RF MEMS phase shifters for phased array applications," *IEEE Microwave Guided Wave Lett.*, vol. 9, pp. 517–519, Dec. 1999.
[5] J. K. Smith, F. W. Hopwood, and K. A. Leahy, "MEM switch technology in radar," in *Proc. IEEE Radar*, Alexandria, VA, May 7–12, 2000, pp. 193–198.

[6] G. M. Rebeiz, G.-L. Tan, and J. S. Hayden, "RF MEMS phase shifters: Design and applications," *IEEE Microwave Mag.*, vol. 3, pp. 72–81, June 2002.

[7] R. C. Johnson and H. Jasik, *Antenna Engineering Handbook*, 2nd ed. New York: McGraw-Hill, 1984.

[8] M. Kim, J. B. Hacker, R. E. Mihailovich, and J. F. DeNatale, "A DC-to-40 GHz four-bit RF MEMS true-time delay network," *IEEE Microwave Wireless Comp. Lett.*, vol. 11, pp. 517–519, Feb. 2001.

**Joseph G. Teti, Jr.** (M'91–SM'01) received the B.S. degree from Drexel University, Philadelphia, PA, in 1985, and the M.S.E. and Ph.D. degrees from the University of Pennsylvania, Philadelphia, in 1989 and 1991, respectively, all in electrical engineering.

From 1985 to 1987, he was a Staff Engineer with Flam and Russell Inc., Horsham, PA. From 1987 to 1992 he was with the Naval Air Development Center (NADC), Warminster, PA. From 1989 to 1991, he was on leave as an NADC Ph.D. Fellow with the Moore School of Electrical Engineering, University of Pennsylvania, Philadelphia. In 1992, he returned to industry and, in 1995, he founded Lambda Science Inc., Wayne, PA, where he is currently the Chief Scientist. His research interests are broad and span topic areas that pertain to the design and application of advanced sensors. He has experience in advanced radar sensor system design and applications that include instrumentation, surveillance, tactical, surface search, high-frequency (HF) over-the-horizon, and synthetic aperture radar. His experience also includes RF hardware, covering areas from devices to antennas, theoretical and applied advanced signal-processing techniques that emphasize the extraction and utilization of available sensor information, and the analysis of propagation and scattering phenomenology for the purposes of mitigation and/or exploitation.

Dr. Teti is a member of several IEEE societies, the Society of Industrial and Applied Mathematics (SIAM), the American Geophysical Union (AGU), the Association of Old Crows (AOC), Tau Beta Pi, and Sigma Xi.

**Francis P. Darreff** (M'62) received the B.S.E.E. and M.S.E.E. degrees from Drexel University, Philadelphia, PA, in 1962 and 1968, respectively.

From 1957 to 1993, he was with the Naval Air Development Center/Naval Air Warfare Center, Warminster, PA, where he contributed to the design, development, and testing of several Navy airborne tactical radar systems and to noncooperative target recognition technology. He also conducted research in synthetic aperture radar (SAR) technology for tactical and oceanographic applications. From 1977 to 1993, he managed the Tactical Radar Branch, which was responsible for developing and expanding Navy tactical radar research and development programs. From 1993 to 2003, he provided technical consulting, concept development, analyses, simulations, and evaluations for state-of-the-art radar technologies in areas of advanced radar systems to several companies [SPC Corporation (1993–1995), Veridian Corporation (1993–2003), Titan Corporation (2001), and Lambda Science Corporation (2002)].